Myeloproliferative disease induced by *TEL-PDGFRB* displays dynamic range sensitivity to *Stat5* gene dosage

Jennifer A. Cain,[1] Zhifu Xiang,[1] Julie O'Neal,[1] Friederike Kreisel,[2] AnnaLynn Colson,[1] Hui Luo,[1] Lothar Hennighausen,[3] and Michael H. Tomasson[1]

[1]Department of Internal Medicine, Division of Oncology, Washington University, Siteman Cancer Center, St Louis, MO; [2]Department of Pathology, Washington University School of Medicine, St Louis, MO; [3]Laboratory of Genetics and Physiology, National Institute of Diabetes and Digestive and Kidney Diseases, National Institutes of Health, Bethesda, MD

Expression of the constitutively activated TEL/PDGFβR fusion protein is associated with the t(5;12)(q33;p13) chromosomal translocation found in a subset of patients with chronic myelomonocytic leukemia. TEL/PDGFβR activates multiple signal transduction pathways in cell-culture systems, and expression of the *TEL-PDGFRB* fusion gene induces myeloproliferative disease (MPD) in mice. We used gene-targeted mice to characterize the contribution of signal transducer and activator of transcription *(Stat)* and *Src* family genes to *TEL-PDGFRB*–mediated transformation in methylcellulose colony and murine bone marrow transduction/transplantation assays. Fetal liver hematopoietic stem and progenitor cells harboring targeted deletion of both *Stat5a* and *Stat5b (Stat5ab$^{null/null}$)* genes were refractory to transformation by *TEL-PDGFRB* in methylcellulose colony assays. Notably, these cell populations were maintained in *Stat5ab$^{null/null}$* fetal livers and succumbed to transformation by *c-Myc.* Surprisingly, targeted disruption of either *Stat5a* or *Stat5b* alone also impaired *TEL-PDGFRB*–mediated transformation. Survival of *TPiGFP→Stat5a$^{-/-}$* and *TPiGFP→Stat5a$^{+/-}$* mice was significantly prolonged, demonstrating significant sensitivity of *TEL-PDGFRB*–induced MPD to the dosage of *Stat5a. TEL-PDGFRB*–mediated MPD was incompletely penetrant in *TPiGFP→Stat5b$^{-/-}$* mice. In contrast, Src family kinases Lyn, Hck, and Fgr and the Stat family member Stat1 were dispensable for *TEL-PDGFRB* disease. Together, these data demonstrate that *Stat5a* and *Stat5b* are dose-limiting mediators of *TEL-PDGFRB*–induced myeloproliferation. (Blood. 2007;109:3906-3914)

Introduction

Chronic myelomonocytic leukemia (CMML) is characterized by dysplastic monocytosis, hypercellular bone marrow, splenomegaly, variable bone marrow fibrosis, and progression to acute myelogenous leukemia (AML). The t(5;12) (q33;p13) chromosomal translocation occurs in a subset of CMML patients. The TEL/PDGFβR fusion protein retains the pointed (PNT) domain found in TEL and the split tyrosine kinase (intracellular) portion of platelet-derived growth factor receptor β (PDGFβR).[1] TEL/PDGFβR self-associates in the cytoplasm as oligomers via the PNT domain and becomes constitutively activated.[2-4] This constitutive tyrosine kinase activity is required for recruitment of SH2-domain signaling intermediates including phosphatidylinositol 3-kinase (PI3K), phospholipase-C γ (PLCγ), SHP2, as well as signal transducers and activators of transcription 1 and 5 (STAT1 and STAT5, respectively).[2,5-7]

A murine bone marrow transduction/transplantation model of *TEL-PDGFRB* is marked by a rapidly fatal myeloproliferative disorder (MPD) that recapitulates aspects of human CMML including leukocytosis, splenomegaly, and extramedullary hematopoiesis.[8] A TEL/PDGFβR mutant with tyrosine to phenylalanine mutations in the juxtamembrane SH2-domain–binding tyrosine residues (TEL/PDGFβR-F2) retains tyrosine kinase activity but does not induce myeloproliferation in mice.[8] TEL/PDGFβR-F2 fails to bind and activate Stat5[6] and, in the context of native PDGFβR, the F2 tyrosines mediate binding and activation of both Src and Stat proteins.[9-11] Therefore Src and Stat are candidate signaling molecules, but their role in mediating disease induced by *TEL-PDGFRB* is unclear. We used gene-targeted mice to characterize the contribution of signal transducer and activator of transcription *(Stat)* and *Src* family genes to *TEL-PDGFRB*–mediated transformation in methylcellulose colony and murine bone marrow transduction/transplantation assays

Materials and methods

Plasmids

TEL-PDGFRB ires *green fluorescent protein (TPiGFP)* was constructed in a murine stem cell virus (MSCV)2.2-ires-*GFP* vector backbone as previously described.[8] *TEL-PDGFRB*-PGK-*Neo (TPNeo)* was generated by subcloning the *TEL-PDGFRB* cDNA into MSCV-*Neo* (Clontech, Mountain View, CA). MSCV-*Myc* was generated as described.[12] *TEL-PDGFRB* ires *c-Src (TPiSrc)* was generated by inserting the *c-Src* cDNA (provided by Sara Courtneidge, Burnham Institute for Medical Research, La Jolla, CA) into MSCV2.2-ires-*GFP,* replacing *GFP* with *c-Src*. The *TEL-PDGFRB* cDNA was then excised from *TPiGFP* and placed into MSCV2.2-ires-*cSrc*. *Stat5^{1*6}* ires *GFP* was created by placing the *Stat5^{1*6}* cDNA (Toshio Kitamura, University of Tokyo, Japan) into MSCV2.2-ires-*GFP. TEL-PDGFRB* ires *Stat5a (TPiStat5a)* was created by placing the *Stat5a* cDNA

Submitted July 19, 2006; accepted December 26, 2006. Prepublished online as *Blood* First Edition Paper, January 11, 2007; DOI 10.1182/blood-2006-07-036335.

The online version of this article contains a data supplement.

The publication costs of this article were defrayed in part by page charge payment. Therefore, and solely to indicate this fact, this article is hereby marked "advertisement" in accordance with 18 USC section 1734.

into MSCV2.2-ires-*GFP* backbone to create MSCV2.2-ires-*mStat5a,* into which the *TEL-PDGFRB* cDNA was subcloned at the *Eco*RI site. *TEL-PDGFRB* ires *Stat5b (TPiStat5b)* was generated by inserting the *mStat5b* cDNA (courtesy of Lothar Hennighausen, NIDDK, Warren Leonard NHLBI, National Institutes of Health, Bethesda, MD) into MSCV2.2-ires-*GFP.* The *TEL-PDGFRB* cDNA was then subcloned into the *Eco*RI site of MSCV2.2-ires-*mStat5b.*

Retrovirus production

Retroviral supernatants were generated by transient transfection of Ecopac (Cell Genesys, Foster City, CA) with MSCV-based retroviral construct using Superfect transfection reagent (Qiagen, Chatsworth, CA) per the manufacturer's instructions. Retroviral supernatants were harvested 48 hours after transfection. To evaluate viral titer of constructs containing *eGFP,* Ba/F3 cells were transduced with retroviral supernatants and GFP expression was determined by flow cytometric detection of GFP positivity. To assess MSCV-*Neo, TPiNeo, TPiStat5a,* and *TPiStat5b* viral titer, 3T3 cells were transduced with retroviral supernatants. 3T3 DNA was isolated and quantitative polymerase chain reaction (PCR) amplication was used to detect psi retroviral sequences compared with control genomic sequences.

Mouse strains

Lyn, Hck, Fgr triply deficient mice[13] were provided by Clifford Lowell (University of California, San Francisco). *Stat1*$^{-/-}$ mice[14] were provided by Robert Schreiber (Washington University, St Louis). Lothar Hennighausen (NIDDK, National Institutes of Health) contributed *Stat5a*$^{-/-}$[15] and *Stat5ab*$^{+/null}$ mice.[16] *Stat5ab*$^{+/null}$ mice were crossed with NIH Black Swiss female mice (Taconic Farms, Hudson, NY). The resulting outbred *Stat5ab*$^{+/null}$ male and female mice were used to generate *Stat5ab*$^{null/null}$, *Stat5ab*$^{null/null}$, and *Stat5ab*$^{null/null}$ fetuses. *Stat5b*$^{-/-}$ mice[17] were acquired from Helen Davey (AgResearch, Hamilton, New Zealand). Assisted speed congenics[18] were used to backcross the targeted *Stat5a* (N3 generation, approximately 94% balb/c) or *Stat5b* (N4 generation, approximately 99% balb/c) allele in singly deficient mice to balb/c (Taconic Farms).

Methylcellulose colony formation

Bone marrow transduction of whole bone marrow (Stat5a and Stat5b singly deficient mouse strains backcrossed to balb/c) was performed as previously described.[8] Briefly, whole bone marrow was harvested from 150 mg/kg 5-fluorouracil–treated mice, and the red blood cells were removed by brief incubation in hypotonic lysis buffer (150 mM NH_4Cl, 10 mM $KHCO_3$, 0.1 mM EDTA, pH 7.4). Unfractionated cells were prestimulated in media containing pen/strep, fetal bovine serum, SCF, IL3, FLT3, and Tpo for 48 hours. Cells were transduced with retroviral supernatants of equivalent titer by 2 rounds of centrifugation at 2500*g* for 90 minutes in the presence of 8 μg/mL polybrene (American Bioanalytical, Natick, MA). Twenty-four hours following the second transduction, cells were washed thrice with cold PBS and resuspended in methylcellulose with cytokines (2×10^4 cells/mL in M3434 methylcellulose; Stem Cell Technologies, Vancouver, BC) or without cytokines (10^5 cells/mL in M3234; Stem Cell Technologies) in the presence or absence of 1 mg/mL G418 (Gibco/Invitrogen, Grand Island, NY; from a 20-mg/mL stock solution in 0.1 M Hepes [Cambrex, Walkersville, MD]) and plated in triplicate. Colonies containing at least 30 cells were counted 10 days after plating. Transduction efficiency for each genotype and experimental condition was determined by plating cells in the presence of cytokines and dividing the average number of G418-resistant colonies per plate by the average number of colonies per plate in a duplicate set of plates not containing G418.

Murine 14.5-dpc fetuses were harvested from *Stat5ab*$^{+/null}$ × *Stat5ab*$^{+/null}$ timed pregnancies and were washed in sterile PBS (Gibco/Invitrogen). Fetal livers were placed into RPMI containing penn/strep and 10% fetal bovine serum and brought to a single-cell suspension by passing through a 27-gauge needle. Red blood cells were lysed as in the paragraph above, and the remaining cells from each fetal liver were resuspended into fetal liver transplant media (RPMI containing pen/strep, 10% fetal bovine serum, 10 ng/mL IL6, 100 ng/mL SCF, 6 ng/mL IL3, 50 ng/mL FLT3, and 10 ng/mL Tpo) and placed at 37°C in 5% CO_2. Fetal liver cell DNA was isolated using Puregene DNA purification kit (Gentra Systems, Minneapolis, MN) and genotyped as described.[16] Cells of each genotype were pooled and replated in fetal liver transplant media and incubated at 37°C in 5% CO_2. Beginning 36 hours after harvest, cells were transduced every 6 hours with retroviral supernatants of equivalent titer by centrifugation at 2500*g* for 10 minutes in the presence of 8 μg/mL polybrene (American Bioanalytical) for a total of 4 transductions. Twenty-four hours following the final transduction, cells were washed and plated in methylcellulose as described in the preceding paragraph. Colonies containing at least 30 cells were counted 10 days after plating. Transduction efficiency was determined as described above for *TPNeo* and MSCV-*Neo* experiments, while detection of GFP-positive cells by flow cytometry immediately prior to plating cells in methylcellulose was used to evaluate MSCV-*Myc* transduction efficiency.

Retroviral transduction and transplantation

Transduction and transplantation were performed as previously described.[8] Syngeneic recipient mice were lethally irradiated and were injected with 10^6 bone marrow cells in 750 μL Hanks buffered saline solution via lateral tail-vein injection. Doses of irradiation were as follows: *Lyn*$^{-/-}$*Hck*$^{-/-}$*Fgr*$^{-/-}$: 450 cGy C57/Black6 (Taconic Farms); *Stat1*$^{-/-}$: 1000 cGy C57BL/6 × 129S6/SvEv F1 (B6129; Taconic Farms); outbred *Stat5a*$^{-/-}$: 1000 cGy B6129 (Taconic Farms); balb/c backcrossed *Stat5a*$^{-/-}$: 900 cGy wild-type littermate control; outbred *Stat5b*$^{-/-}$: 1000cGy B6129 (Taconic Farms); balb/c backcrossed *Stat5b*$^{-/-}$: 900 cGy wild-type littermate control.

Mouse analysis

Peripheral blood was obtained from the saphenous vein of moribund mice and blood counts were analyzed (Hemavet; CDC Technologies, Oxford, CT). Moribund mice were killed and spleen weight was recorded. Heart, lungs, tibia, spleen, kidney, and liver were fixed using 10% neutral buffered formalin (Sigma-Aldrich, St Louis, MO). Slides of peripheral blood and formalin-fixed tissue were hematoxylin and eosin (H&E) stained and imaged using an Olympus BX40 F4 microscope with an oil-immersion 50×/0.90 or 100×/1.30 objective lens (Olympus Optical, Tokyo, Japan) using an Olympus DP70 digital camera using DPController software (Olympus Optical). Statistical analyses were generated with StatView (SAS Institute, Cary, NC). Kaplan-Meier plots were generated using Excel (Microsoft, Redmond, WA).

Flow cytometry

Bone marrow cells and splenocytes were brought to a single-cell suspension in RPMI-1640 (Cambrex) and the red blood cells were removed by brief incubation in hypotonic lysis buffer. Cells were washed once with flow buffer (PBS, 0.5% BSA, 0.1 mM EDTA), and 10^6 cells were resuspended in 100 μL flow buffer and incubated with 1 μL each of the antibodies recognizing murine Gr-1 and Mac-1 conjugated to PE and PECy7, respectively (eBiosciences, San Diego, CA) for 1 hour on ice. Cells were then washed twice with flow buffer and resuspended in 250 μL flow buffer. Data were collected using either MoFlo (Dako, Carpinteria, CA) or Cytomics FC 500 (Beckman Coulter, Fullerton, CA). Figures were prepared using FloJo software (Tree Star, San Carlos, CA).

Progenitor analysis methods

As described under "Methylcellulose colony formation." 14.5-dpc fetal liver cells were harvested, brought to a single-cell suspension in PBS (Gibco/Invitrogen), and stored at 4°C during DNA isolation (REDExtract; Sigma-Aldrich) and genotyping (as described[16]). Unfractionated fetal liver cells of each genotype were pooled into *Stat5ab*$^{-/-}$ (n = 8 fetal livers), *Stat5ab*$^{+/-}$ (n = 6), and *Stat5ab*$^{+/+}$ (n = 7) cohorts, filtered through a 50-μM filter (Partec, Münster, Germany), and stained for flow cytometric analysis of progenitor populations as described.[19] Antibody staining for lineage markers was performed using FITC-conjugated CD3e (145-2C11), CD4 (RM4-5), CD8a (53-6.7), CD19 (1D3), CD45R (RA3-6B2), and GR1 (RB6-8C5) acquired from BD PharMingen (San Diego, CA) and TER119 (TER-119) and CD127 (A7R34) from eBiosciences. Cells were also stained

using biotin-CD34 (RAM34), PE-streptavidin, APC-Sca-1 (D7), PE-Cy7-CD16/32 (93), and APC-Alexa750-CD117 (2B8) antibodies obtained from eBiosciences. Data were collected from 5×10^6 cells per genotype using MoFlo flow cytometer (Dako), and figures were prepared using FloJo software (Tree Star).

Results

Stat5 is required in primary murine hematopoietic cells for *TEL-PDGFRB*–mediated growth

Mice harboring targeted deletions of both *Stat5a* and *Stat5b* genes *(Stat5ab$^{null/null}$)* rarely survive past weaning.[16,20] Therefore, we evaluated *TEL-PDGFRB* transformation in methylcellulose colony formation assays using fetal liver hematopoietic stem cells (HSCs) and progenitor cells. We transduced unfractionated *Stat5ab$^{+/+}$*, *Stat5ab$^{+/null}$*, and *Stat5ab$^{null/null}$*[16] fetal liver cells with retroviral supernatants encoding either *TEL-PDGFRB* with a neomycin resistance cassette *(TPNeo)* or Neo alone (MSCV-*Neo*) and plated them in methylcellulose in the absence of cytokines. Transduction efficiency was equivalent among *Stat5ab$^{+/+}$*, *Stat5ab$^{+/null}$*, and *Stat5ab$^{null/null}$* cells. *TEL-PDGFRB* induced G418-resistant colony formation in *Stat5ab$^{+/+}$* and *Stat5ab$^{+/null}$* cells. In contrast, *Stat5ab$^{null/null}$* cells were completely resistant to *TEL-PDGFRB*–mediated transformation (Figure 1A). MSCV-*Neo* did not cause cytokine independent colony formation in *Stat5ab$^{+/+}$*, *Stat5ab$^{+/null}$*, or *Stat5ab$^{null/null}$* cells (data not shown). As a positive control for the transduction of hematopoietic stem and progenitor cells from these mice, we transduced *Stat5ab$^{+/+}$* and *Stat5ab$^{null/null}$* cells with *c-Myc*. *c-Myc* readily transformed both *Stat5ab$^{+/+}$* and *Stat5ab$^{null/null}$* cells to generate cytokine-independent colonies (Figure 1A), confirming efficient retroviral transduction of Stat5-deficient cells.

We were impressed by the dramatic reduction of *TEL-PDGFRB*–induced cytokine-independent colonies in the absence of *Stat5* and were concerned that our data might be explained by reduced hematopoietic stem and progenitor cells in these mutant mice. To further assess the presence and quantity of hematopoietic stem and progenitor cells in *Stat5ab$^{null/null}$* fetal livers, we performed multiparameter immunophenotypic analysis using high-speed flow cytometry.[19] Less mature, lineage-negative cells were twice as prevalent among *Stat5ab$^{null/null}$* fetal liver cells compared with *Stat5ab$^{+/+}$* cells (data not shown). Among lineage-negative cells, there were equivalent numbers of HSC (KLS) cells present in *Stat5ab$^{null/null}$* and *Stat5ab$^{+/+}$* fetal livers (Figure 2A). Together, these data indicate that HSCs are twice as prevalent among *Stat5ab$^{null/null}$* fetal liver cells, consistent with the findings of other investigators.[21] The incidence of common myeloid progenitor (CMP) was the same among *Stat5ab$^{null/null}$*, *Stat5ab$^{+/null}$*, and *Stat5ab$^{+/+}$* Kit$^+$Lin$^-$Sca$^-$ fetal liver cells (Figure 2A). Megakaryocyte-erythrocyte progenitor (MEP) populations were moderately increased in *Stat5ab$^{null/null}$* fetal liver cells (Figure 2A). Notably, granulocyte-monocyte progenitors (GMPs) were markedly decreased (Figure 2A). When evaluated as subsets of all fetal liver cells, immunophenotypically defined hematopoietic stem cell–enriched and progenitor populations were moderately increased in *Stat5ab$^{null/null}$* fetal liver cells compared with wild-type littermate controls (summarized in Figure 2B).

We plated transduced fetal liver cells in methylcellulose containing SCF, IL3, IL6, and EPO to determine if *Stat5ab$^{null/null}$* progenitor cells form colonies in methylcellulose. MSCV-*Neo*–transduced *Stat5ab$^{null/null}$* cells generated half the number of colonies found on *Stat5ab$^{+/+}$* plates (Figure 2C). Expression of *TEL-PDGFRB* rescued the colony formation defect in *Stat5ab$^{null/null}$* fetal liver cells, suggesting that TEL-PDGFβR activated Stat5-independent signaling pathways to restore colony formation capacity to that of *Stat5ab$^{+/+}$* cells (data not shown). Taken together, these data suggest that the inability of *TEL-PDGFRB* to transform *Stat5ab$^{null/null}$* fetal liver cells was not due to the absence of HSC or progenitor-cell populations.

Stat5a and Stat5b share 96% similarity on an amino acid level[22] and serve largely redundant functions in hematopoiesis.[15-16,17,23] Therefore, we hypothesized that *TEL-PDGFRB*–mediated transformation would not be affected by deficiency of either Stat5a or Stat5b alone (ie, either *Stat5a$^{-/-}$Stat5b$^{+/+}$* or *Stat5a$^{+/+}$Stat5b$^{-/-}$*). *Stat5a$^{-/-}$* and *Stat5b$^{-/-}$* mice have no defects in basal hematopoiesis[15,17] (and data not shown), however Stat5a and Stat5b possess distinct DNA-binding specificities[24-25] and have unique roles in response to high doses of Flt3 ligand.[26] We tested the role of individual *Stat5* genes in *TEL-PDGFRB* transformation using methylcellulose colony assays and bone marrow transduction/transplantation assays. We transduced whole bone marrow cells

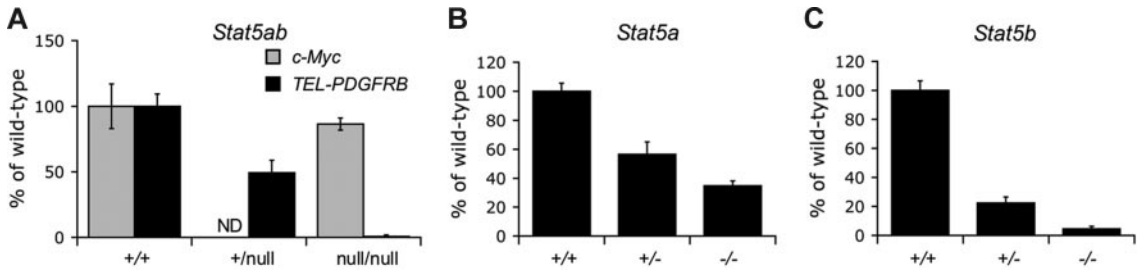

Figure 1. *Stat5* is required in primary murine hematopoietic cells for *TEL-PDGFRB*–mediated growth. (A) Cytokine-independent colony formation of 14.5-dpc fetal liver cells expressing either *TEL-PDGFRB* or *c-Myc*. Data shown are the mean percentage of colonies formed by *Stat5ab$^{null/null}$* and *Stat5ab$^{+/null}$* cells relative to *Stat5ab$^{+/+}$* cells for a given experimental condition. Error bars represent standard deviation. *TPNeo* induced formation of 195 ± 18 *Stat5ab$^{+/+}$*, 194 ± 19 *Stat5ab$^{+/null}$*, and 3 ± 1 *Stat5ab$^{null/null}$* G418-resistant colonies per 10^5 transduced fetal liver cells. Positive control *c-Myc* induced formation of 159 ± 8 colonies per 10^5 *Stat5ab$^{null/null}$* fetal liver cells plated and 184 ± 31 colonies in *Stat5ab$^{+/+}$* cells. Cells transduced with negative control MSCV-*Neo* did not form colonies in the absence of cytokines (data not shown). Transduction efficiency of *Stat5ab$^{+/+}$* and *Stat5ab$^{null/null}$* fetal liver cells with MSCV-*Myc* was 14% and 12% for 2 independent experiments. For *TPNeo* and MSCV-*Neo,* transduction efficiency of *Stat5ab$^{+/+}$* cells averaged 25% ± 15% and *Stat5ab$^{null/null}$* cells averaged 45% ± 16% for 7 independent transductions of each genotype. (B) *TEL-PDGFRB* induced cytokine independent colony formation in *Stat5a$^{+/+}$* (469 ± 26 colonies per 10^5 transduced cells), *Stat5a$^{+/-}$* (266 ± 40), and *Stat5a$^{-/-}$* (163 ± 16) whole bone marrow cells. Data shown are the mean percentage of colonies formed by *Stat5a$^{-/-}$* and *Stat5a$^{+/-}$* cells relative to *Stat5a$^{+/+}$* cells for a given experimental condition. Error bars represent standard deviation. Transduction efficiency of *Stat5a$^{-/-}$* cells averaged 98% ± 17% and 93% ± 18% for *Stat5a$^{+/+}$* bone marrow cells in 3 independent transductions. (C) *TEL-PDGFRB* induced cytokine-independent colony formation in *Stat5b$^{+/+}$* (602 ± 39 colonies per 10^5 transduced cells), *Stat5b$^{+/-}$* (135 ± 25), and *Stat5b$^{-/-}$* (27 ± 11) whole bone marrow cells. Data shown are the mean percentage of colonies formed by *Stat5b$^{-/-}$* and *Stat5b$^{+/-}$* cells relative to *Stat5b$^{+/+}$* cells for a given experimental condition. Error bars represent standard deviation. Transduction efficiency of *Stat5b$^{-/-}$* cells was 99% and 81% for *Stat5b$^{+/+}$* bone marrow cells. (*TPNeo* indicates *TEL-PDGFRB*-PGK *Neo;* MSCV-*Myc,* MSCV-*c-Myc* ires GFP; and ND, not done.)

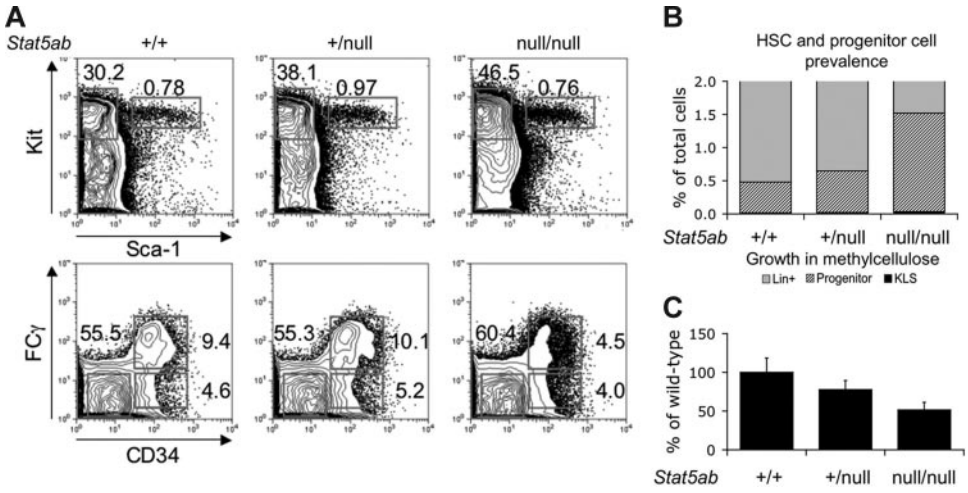

Figure 2. Hematopoietic stem and progenitor-cell populations are preserved in fetal livers of *Stat5ab*$^{null/null}$ mice. (A) Flow cytometric analysis of *Stat5ab*$^{null/null}$, *Stat5ab*$^{+/null}$, and *Stat5ab*$^{+/+}$ 14.5-dpc fetal livers for early hematopoietic cells. Top panel shows Kit and Sca-1 expression of lineage-negative fetal liver cells. Bottom panel shows CMP (FcγR^{lo}CD34^{+}), MEP (FcγR^{lo}CD34^{-}), and GMP (FcγR^{hi}CD34^{+}) populations, with percentage of Kit^{+}Lin^{-}Sca^{-} falling into each progenitor population as indicated. (B) Proportion of cells that is identified as either KLS (black), progenitors (CMPs, MEPs, or GMPs, diagonal stripes), or lineage-committed (gray) hematopoietic cells within *Stat5ab*$^{+/+}$, *Stat5ab*$^{+/null}$, and *Stat5ab*$^{null/null}$ 14.5-dpc fetal livers as determined by flow cytometric detection of cell-surface markers. (C) Cytokine-dependent colony formation of vector-transduced 14.5-dpc fetal liver cells when cells were plated in the presence of SCF, IL3, IL6, and EPO. Data shown are the mean percentage of colonies formed by *Stat5ab*$^{null/null}$ and *Stat5ab*$^{+/null}$ cells relative to *Stat5ab*$^{+/+}$ cells. Error bars represent standard deviation. Vector control *Stat5ab*$^{+/+}$ cells generated 688 ± 18 G418-resistant colonies per 10^5 transduced fetal liver cells, while *Stat5ab*$^{+/null}$ and *Stat5ab*$^{null/null}$ cells formed 535 ± 12 and 355 ± 10 colonies. *TPNeo*-transduced *Stat5ab*$^{+/+}$, *Stat5ab*$^{+/null}$, and *Stat5ab*$^{null/null}$ cells formed 337 ± 33, 559 ± 43, and 321 ± 30 G418 colonies, respectively. Transduction efficiency of *Stat5ab*$^{+/+}$ cells averaged 25% ± 15% and *Stat5ab*$^{null/null}$ cells averaged 45% ± 16% for 7 independent transductions of each genotype. (KLS indicates Kit^{+}Sca^{+}Lin^{-}; CMP, common myeloid progenitor; MEP, megakaryocyte-erythrocyte progenitor; and GMP, granulocyte-monocyte progenitor.)

harboring targeted disruption of either *Stat5a* or *Stat5b* with either *TPNeo* or MSCV-*Neo* retroviral supernatants and plated them in the absence of cytokines. *TEL-PDGFRB* transformed wild-type cells to cytokine-independent growth (Figure 1B-C). Remarkably, there was a downward trend of *TEL-PDGFRB*–transformed colonies when either *Stat5a*$^{+/-}$ singly targeted or *Stat5b*$^{+/-}$ singly targeted bone marrow cells were used. Finally, deficiency in either Stat5a or Stat5b alone caused a significant reduction in the incidence of *TEL-PDGFRB*–transformed colonies (Figure 1B-C), indicating that both Stat5a and Stat5b contribute to transformation. Transduction efficiency was equivalent in all cohorts. Taken together, these data demonstrate that Stat5 is critical to *TEL-PDGFRB*–induced transformation.

Stat5a gene dosage mediates the latency of *TEL-PDGFRB*–induced myeloproliferation

Given the surprising attenuation of *TEL-PDGFRB*–mediated transformation in the absence of *Stat5a,* we sought to determine the impact of Stat5a deficiency upon the myeloproliferative disease induced by *TEL-PDGFRB* in vivo. Unlike *Stat5ab*$^{null/null}$ mice, Stat5a-deficient mice have abnormal lactogenesis, but no defects in steady-state myelopoiesis,[15] and can be used as donors for bone marrow transplant assays. We assessed the relative contribution of the *Stat5a* gene to *TEL-PDGFRB*–mediated transformation in bone marrow transduction/transplantation experiments using Stat5a singly deficient *(Stat5a*$^{-/-}$*),* heterozygous *(Stat5a*$^{+/-}$*),* and wild-type *(Stat5a*$^{+/+}$*)* donor mice with retroviral supernatants encoding *TEL-PDGFRB* with *eGFP (TPiGFP).* Survival of *TPiGFP→Stat5a*$^{-/-}$ mice was significantly prolonged in comparison with *TPiGFP→Stat5a*$^{+/+}$ mice (144 versus 31 days, $P < .001$; Figure 3A). Surprisingly, disease latency in *TPiGFP→Stat5a*$^{+/-}$ mice was similar to that of *TPiGFP→Stat5a*$^{-/-}$ mice (145 versus 144 days, $P = .867$) and was significantly prolonged compared with survival of *TPiGFP→Stat5a*$^{+/+}$ mice (145 versus 31 days, $P < .001$; Figure 3A). Therefore, the latency of *TEL-PDGFRB*–induced disease was significantly affected by the loss of even a single wild-type *Stat5a* allele.

Despite significant prolongation of survival, all mice eventually succumbed to disease. We characterized *TEL-PDGFRB* disease in each *Stat5a* genotype cohort at time of death. Histopathologic analysis of *TPiGFP→Stat5a*$^{+/+}$ mice revealed severe extramedullary hematopoiesis with accumulation of large numbers of mature myeloid cells in the liver sinusoids and perivascular regions of the liver and profoundly disrupted splenic architecture (data not shown). Blood vessels and capillaries were filled with granulocytes with multifocal congestion and hemorrhage in the lungs of *TPiGFP→Stat5a*$^{+/+}$ mice. Consistent with the prolonged survival of both *TPiGFP→Stat5a*$^{-/-}$ and *TPiGFP→Stat5a*$^{+/-}$ mice, only mild extramedullary hematopoiesis was detected in both *TPiGFP→Stat5a*$^{-/-}$ and *TPiGFP→Stat5a*$^{+/-}$ mice (data not shown), although all cohorts had splenomegaly. There were slight to moderate accumulations of granulocytes in the livers and diffuse expansion of granulocytes in the spleens of both *TPiGFP→Stat5a*$^{-/-}$ and *TPiGFP→Stat5a*$^{+/-}$ cohorts at time of death due to disease (data not shown). Well-differentiated granulocytes infiltrated the lungs of *TPiGFP→Stat5a*$^{-/-}$ and *TPiGFP→Stat5a*$^{+/-}$ recipient mice, with mild to moderate multifocal congestion in the lungs. *TPiGFP→Stat5a*$^{+/+}$ mice displayed severe leukocytosis, while leukocytosis in *TPiGFP→Stat5a*$^{+/-}$ and *TPiGFP→Stat5a*$^{-/-}$ mice was significantly reduced (median WBC, 29 × 10^9/L [29 000/μL] and 28 × 10^9/L [28 000/μL], respectively; Figure 3B). Taken together, these data show that *TEL-PDGFRB*–induced MPD was attenuated in both disease latency and severity in *TPiGFP→Stat5a*$^{-/-}$ and *TPiGFP→Stat5a*$^{+/-}$ mice, suggesting that *TEL-PDGFRB*–induced MPD was significantly reduced by absence or haploinsufficiency of *Stat5a.*

While transduction efficiency was equivalent among *Stat5a*$^{-/-}$, *Stat5a*$^{+/-}$, and *Stat5a*$^{+/+}$ cells in a methylcellulose assay for *TEL-PDGFRB*–mediated transformation, we sought to confirm that we had efficiently transduced and transplanted *Stat5a*$^{-/-}$ and

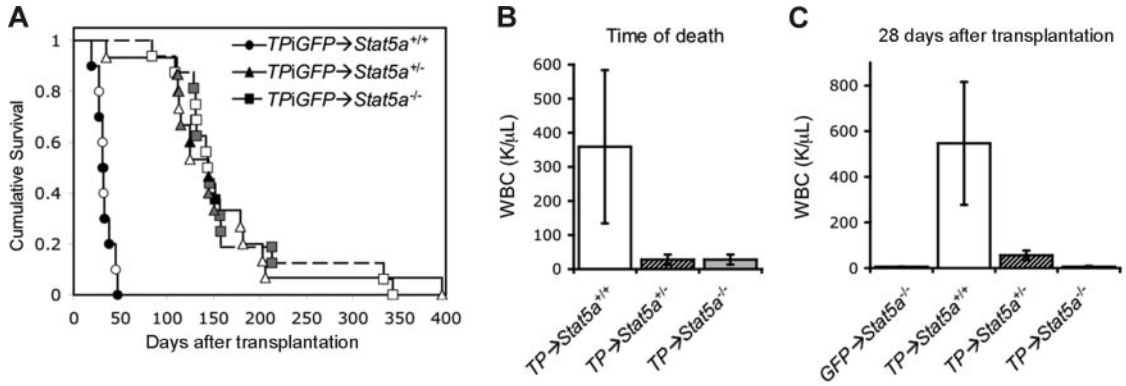

Figure 3. *Stat5a* gene dosage mediates the latency of *TEL-PDGFRB*–induced myeloproliferation. (A) Kaplan-Meier plot shows survival of recipient mice when *TEL-PDGFRB* is expressed in bone marrow cells harboring homozygous or heterozygous inactivation of *Stat5a*. *TPiGFP→Stat5a*$^{+/+}$ mice (circles) developed severe MPD (spleen weight median, 790 ± 90 mg; range, 620-910 mg; n = 6). *TPiGFP→Stat5a*$^{+/-}$ mice (△) developed moderate or severe MPD (spleen weight median, 770 ± 300 mg; range, 350-1120 mg; n = 7). *TPiGFP→Stat5a*$^{-/-}$ mice (squares) developed moderate MPD with splenomegaly (spleen weight, 710 ± 550 mg; range, 350-2070 mg; n = 8) and leukocytosis. Black shapes indicate death due to severe (fatal) MPD marked by leukocytosis and splenomegaly (WBC, > 50 × 10^9/L [50 000/μL] and spleen weight, > 450 mg) at time of death due to disease. Shaded shapes represent moderate MPD (WBC, > 15 × 10^9/L [15 000/μL] and/or spleen weight, > 450 mg) at time of death due to disease. Open shapes indicate animal found dead. (B) Median peripheral blood cell count at time of death due to disease. Error bars represent standard deviation. *TEL-PDGFRB* induced severe leukocytosis in *TPiGFP→Stat5a*$^{+/+}$ mice (359 ± 225 × 10^9/L [359 000 ± 225 000/μL]; range, 60-737 × 10^9/L [60 000-737 000/μL]; n = 6) and moderate leukocytosis in *TPiGFP→Stat5a*$^{+/-}$ mice (28 ± 15 × 10^9/L [28 000 ± 15 000/μL]; range, 12-131 × 10^9/L [12 000-131 000/μL]; n = 7) as well as *TPiGFP→Stat5a*$^{-/-}$ mice (29 ± 27 × 10^9/L [29 000 ± 27 000/μL];range, 10-94 × 10^9/L [10 000-94 000/μL]; n = 8). (C) Three mice from each cohort were analyzed 28 days after transplantation. Median of peripheral blood counts is shown. Error bars represent standard deviation. Peripheral blood counts of *GFP→Stat5a*$^{-/-}$ control mice are also shown. (TPiGFP indicates *TEL-PDGFRB* ires *eGFP;* MPD, myeloproliferative disease; and WBC, peripheral white blood cell count.)

Stat5a$^{+/+}$ cells in our in vivo model. To address the possibility that pretreatment with 5-FU reduces the *Stat5a*$^{-/-}$ transduction/transplantation target population relative to that in *Stat5a*$^{+/+}$ cells, we transduced *Stat5a*$^{-/-}$ donor cells with retroviral supernatants encoding a constitutively activated Stat5a, *Stat5*$^{1*6.27}$. As expected, *Stat5*^{1*6}→*Stat5a*$^{-/-}$ recipient mice developed a rapidly fatal disease (median survival, 19 ± 1 days; data not shown), similar to disease seen in wild-type mice.[28] We further verified equivalent integration of retroviral construct among transplanted *Stat5a*$^{-/-}$ and *Stat5a*$^{+/+}$ donor cells in *TPiGFP→Stat5a*$^{-/-}$ and *TPiGFP→Stat5a*$^{+/+}$ recipient mice as detected by linear amplification-mediated (LAM)–PCR (Figure S2, available on the *Blood* website; see the Supplemental Figures link at the top of the online article). These data are consistent with a previous report demonstrating that 5-FU affects *Stat5a*$^{-/-}$ and *Stat5a*$^{+/+}$ myeloid donor-cell populations equally and that clonal integrations of *Stat5a*$^{-/-}$ and *Stat5a*$^{+/+}$ transduced and transplanted cells are equivalent.[29]

We were struck by the dramatic reduction in disease severity afforded by loss of a single *Stat5a* allele in *TPiGFP→Stat5a*$^{+/-}$ mice. We analyzed *TPiGFP→Stat5a*$^{+/+}$, *TPiGFP→Stat5a*$^{+/-}$, and *TPiGFP→Stat5a*$^{-/-}$ mice 28 days after transplantation to assess the effects of *Stat5a* deficiency and haploinsufficiency on *TEL-PDGFRB*–induced myeloproliferation early after transduction/transplantation. All *TPiGFP→Stat5a*$^{+/+}$ mice developed severe MPD (median WBC, 547 × 10^9/L [547 000/μL]; spleen weight, 860 mg; Figure 3C), as expected. *TEL-PDGFRB*–mediated myeloproliferation was blunted in *TPiGFP→Stat5a*$^{+/-}$ mice (median WBC, 56 × 10^9/L [56 000/μL]; spleen weight, 790 mg) (Figure 3C). *TPiGFP→Stat5a*$^{-/-}$ mice showed no evidence of disease (median WBC, 5 × 10^9/L [5000/μL]; spleen weight, 53 mg; Figure 3C). These data support the conclusion that *TEL-PDGFRB*–induced myeloproliferation responds significantly to the loss of even a single *Stat5a* allele.

TEL-PDGFRB–mediated MPD is incompletely penetrant in the absence of *Stat5b*

TPiGFP→Stat5a$^{+/-}$ and *TPiGFP→Stat5a*$^{-/-}$ mice were protected against *TEL-PDGFRB*–mediated MPD despite intact *Stat5b*. To directly address a role for *Stat5b* in *TEL-PDGFRB*–mediated MPD, we used donor mice with homozygous inactivation of *Stat5b*. Both *TPiGFP→Stat5b*$^{+/+}$ and *TPiGFP→Stat5b*$^{-/-}$ mice developed fatal MPD (Figure 4A) marked by leukocytosis and extramedullary hematopoiesis. Mature myeloid cells invaded the spleens of both *TPiGFP→Stat5b*$^{+/+}$ and *TPiGFP→Stat5b*$^{-/-}$ mice as detected by both flow cytometric (Figure 4B) and histopathologic (Figure 4C) analysis. Further, histopathologic analysis revealed that sheets of these mature myeloid cells (predominately mature neutrophils) disrupted splenic architecture and destroyed the normal pattern of white pulp nodules in a matrix of red pulp evident in *eGFP* control mice (Figure 4C). Mature myeloid cells infiltrated sinusoids and perivascular regions of the liver in both *TPiGFP→Stat5b*$^{-/-}$ and *TPiGFP→Stat5b*$^{+/+}$ mice, unlike in their *eGFP* control mice counterparts (Figure 4C). The bone marrow of both cohorts was hypercellular, with atypical myeloid cells observed by histopathologic analysis (data not shown).

Our data demonstrated that *Stat5b* was not absolutely required for *TEL-PDGFRB*–mediated MPD. However, we noted that 5 of 13 *TPiGFP→Stat5b*$^{-/-}$ mice appeared to escape rapidly fatal MPD induced by *TEL-PDGFRB* and were longer lived (Figure 4A). We confirmed equivalent GFP expression in *TPiGFP→Stat5b*$^{+/+}$ and *TPiGFP→Stat5b*$^{-/-}$ recipient bone marrow cells and splenocytes (data not shown), showing that transduced and transplanted cells persist in surviving *TPiGFP→Stat5b*$^{-/-}$ mice. We evaluated myeloproliferation in the longer-lived subset of *TPiGFP→Stat5b*$^{-/-}$ mice. We assessed these mice by gross and microscopic pathology, peripheral blood cell count, and flow cytometric analysis of spleen and bone marrow. However, we did not detect significant myeloproliferation in long-lived (> 100 days after transplantation) *TPiGFP→Stat5b*$^{-/-}$ mice by histopathology and detected only normal to mildly elevated peripheral blood cell counts in 2 of 2 mice analyzed (mean WBC, 11 × 10^9/L [11 000/μL]). However, we noted that leukocytosis at time of death due to disease was somewhat reduced in *TPiGFP→Stat5b*$^{-/-}$ mice (median WBC, 80 × 10^9/L [80 000/μL]) compared with *TPiGFP→Stat5b*$^{+/+}$ littermate controls (median WBC, 213 × 10^9/L [213 000/μL]). While

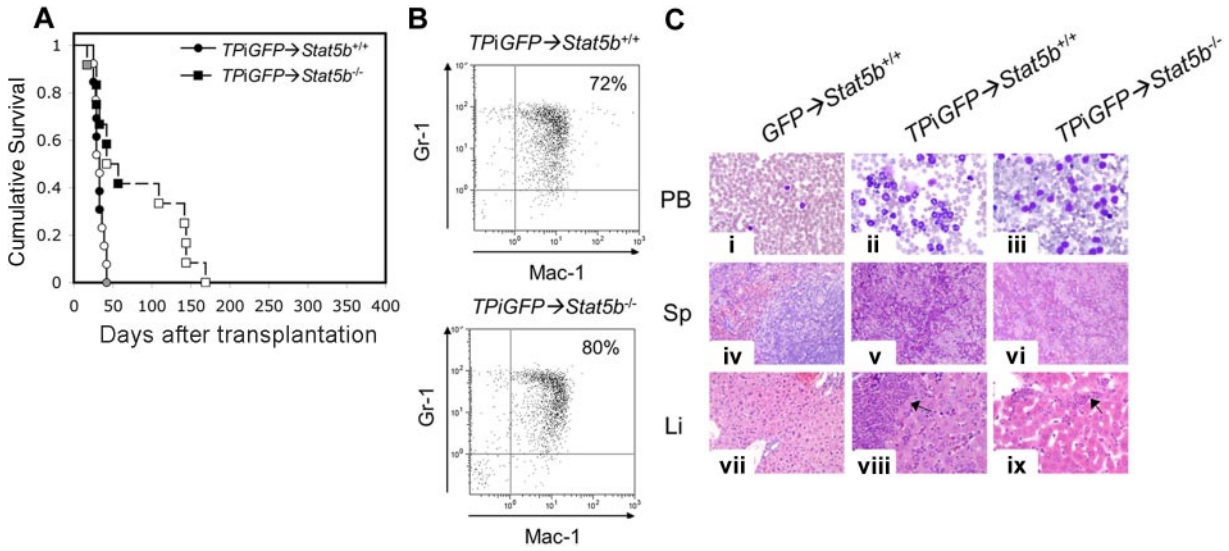

Figure 4. Severity and penetrance of *TEL-PDGFRB*–induced myeloproliferation are reduced in the absence of Stat5b. (A) Kaplan-Meier plot shows survival of recipient mice when *TEL-PDGFRB* is expressed in bone marrow cells harboring targeted deletion of *Stat5b* (*TPiGFP→Stat5b*$^{-/-}$, squares) or wild-type control bone marrow cells (*TPiGFP→Stat5b*$^{+/+}$, ○). *TPiGFP→Stat5b*$^{+/+}$ mice developed severe MPD (spleen weight median, 890 ± 274 mg; range, 670-1460 mg [n = 6]; WBC median, 139 ± 87 × 10^9/L [139 000 ± 87 000/μL]; range, 13-237 × 10^9/L [13 000-237 000/μL] [n = 6]; median survival ± standard error, 33 ± 2.9 days). Severe MPD was detected in 5 of 7 *TPiGFP→Stat5b*$^{-/-}$ mice at time of death due to disease (spleen weight median, 1220 ± 401 mg; range, 420-1440 mg [n = 7]; WBC median, 103 ±151 × 10^9/L [103 000 ± 151 000/μL]; range, 6-446 × 10^9/L [6000-446 000/μL] [n = 7]; median survival ± standard error, 57 ± 60.2 days). Experiment was performed twice, once in the original outbred strain with wild-type littermate control and again with the targeted *Stat5b* allele backcrossed to balb/c resulting in similar disease latency and severity. Black shapes indicate death due to severe MPD marked by leukocytosis and splenomegaly (WBC, > 50 × 10^9/L [50 000/μL] and spleen weight, > 450 mg) at time of death due to disease. Shaded shapes represent moderate MPD (WBC, > 15 × 10^9/L [15 000/μL] and/or spleen weight, > 450 mg) at time of death due to disease. Open shapes indicate animal found dead. GFP was detected in bone marrow, spleen, and peripheral blood of *TPiGFP→Stat5b*$^{-/-}$ (37% ± 4% [n = 7]; 50% ± 15% [n = 7]; and 58% ± 32% [n = 7], respectively) and *TPiGFP→Stat5b*$^{+/+}$ (44% [n = 1]; 50% ± 15% [n = 3]; and 58% ± 32% [n = 3], respectively) recipient mice (data not shown). (B) Flow cytometric detection of mature myeloid (Gr-1$^+$Mac-1$^+$) cells in the spleens of both *TPiGFP→Stat5b*$^{+/+}$ and *TPiGFP→Stat5b*$^{-/-}$ mice 33 days after transplantation. (C) Microscopic images of representative mice at time of death (*GFP→Stat5b*$^{+/+}$, 151 days after transplantation; *TPiGFP→Stat5b*$^{+/+}$, 29 days after transplantation; and *TPiGFP→Stat5b*$^{-/-}$, 29 days after transplantation). Panels show Wright-Giemsa–stained smears of peripheral blood (Ci-iii; 100×), and H&E–stained histologic sections of spleen (Civ-vi; 20×) and liver (Cvii-ix; 40×). These illustrate a normal morphology of peripheral blood, spleen, and liver in the *GFP→Stat5b*$^{+/+}$ group, whereas both *TPiGFP→Stat5b*$^{+/+}$ and *TPiGFP→Stat5b*$^{-/-}$ show marked leukocytosis of maturing neutrophils in the peripheral blood, pronounced red pulp expansion by myeloid hyperplasia composed of predominantly maturing forms in the spleen, and sinusoidal and perivascular infiltrates of maturing granulocytic cells in the liver. Arrows indicate clusters of maturing myeloid cells in the liver. (TPiGFP indicates *TEL-PDGFRB* ires *eGFP;* MPD, myeloproliferative disease; WBC, peripheral white blood cell count; PB, peripheral blood; Sp, spleen; and Li, liver.)

dispensable for *TEL-PDGFRB*–induced myeloproliferation, *Stat5b* was required for complete penetrance of rapidly fatal disease.

Stat5b can restore MPD when coexpressed with *TEL-PDGFRB* in Stat5a-deficient bone marrow cells

We found significant differences in disease latencies between *TPiGFP→Stat5a*$^{-/-}$ and *TPiGFP→Stat5a*$^{+/+}$ mice. To address the possibility that Stat5a and Stat5b are distinct in their ability to transmit myeloproliferative signals in response to *TEL-PDGFRB,* we repeated murine bone marrow transduction/transplantation assays using retroviral constructs to coexpress *TEL-PDGFRB* with either *Stat5a (TPiStat5a)* or *Stat5b (TPiStat5b)* (Figure S1). We transduced unfractionated bone marrow cells harvested from *Stat5a*$^{-/-}$ or *Stat5a*$^{+/-}$ mice with *Stat5* add-back constructs and evaluated mice for survival and evidence of disease. *TEL-PDGFRB*–mediated myeloproliferation was restored by either *Stat5a* or *Stat5b* expression in *TPiStat5a→Stat5a*$^{-/-}$, *TPiStat5a→Stat5a*$^{+/-}$, and *TPiStat5b→Stat5a*$^{-/-}$ mice, with all cohorts developing fatal MPD characterized by leukocytosis and extramedullary hematopoiesis (Table 1; Figure S3). In these add-back experiments, Stat5a and Stat5b appeared to be equivalent in their ability to restore MPD with similar disease latencies (*TPiStat5a→Stat5a*$^{-/-}$ 96 days versus *TPiStat5b→Stat5a*$^{-/-}$ 97 days, $P = .793$). Also, *TPiStat5a→Stat5a*$^{+/-}$ mice developed MPD (median WBC, 66 × 10^9/L [66 000/μL]; spleen weight, 520 mg) with the shortest disease latency (median survival, 28 days versus 31 days in *TPiGFP→Stat5a*$^{+/+}$ mice, $P = .732$), demonstrating again the correlation of disease latency and *Stat5a* gene dosage. Histopathologic analysis of both *TPiStat5a→Stat5a*$^{-/-}$ and *TPiStat5b→Stat5a*$^{-/-}$ mice revealed red pulp expansion with myeloid hyperplasia in the spleen and small clusters of well-differentiated granulocytic cells accumulated in the sinusoids and perivascular regions of the liver (data not shown). These data suggest that both *Stat5a* and *Stat5b* can contribute to *TEL-PDGFRB*–mediated myeloproliferation when expressed at high levels in bone marrow mononuclear cells.

Stat1 and Src family kinases are dispensable for *TEL-PDGFRB*–mediated myeloproliferative disease

We evaluated the contribution of the remaining candidate signaling molecules, the Src family kinases, and Stat1 to *TEL-PDGFRB*–mediated MPD using mice either triply deficient in myelomonocytic Src family kinases Lyn, Hck, and Fgr (*Lyn*$^{-/-}$*Hck*$^{-/-}$*Fgr*$^{-/-}$) or deficient for Stat1 (*Stat1*$^{-/-}$). We transduced unfractionated bone marrow mononuclear cells from *Lyn*$^{-/-}$*Hck*$^{-/-}$*Fgr*$^{-/-}$ or strain-matched wild-type mice with *TPiGFP* retroviral supernatants and transplanted them into lethally irradiated syngeneic recipient mice. We analyzed mice from each cohort for survival and myeloproliferative disease burden at time of death by peripheral blood cell count (WBC), as well as gross and microscopic pathology. All recipient mice (100%) that received *TEL-PDGFRB*–transduced *Lyn*$^{-/-}$*Hck*$^{-/-}$*Fgr*$^{-/-}$ bone marrow cells and either *GFP (TPiGFP→Lyn*$^{-/-}$*Hck*$^{-/-}$*Fgr*$^{-/-}$*)* or *c-Src (TPiSrc→Lyn*$^{-/-}$

Table 1. *Stat5a* and *Stat5b* both restore myeloproliferation when coexpressed with *TEL-PDGFRB* in Stat5a-deficient bone marrow cells

Construct	Phenotype	Median survival, d	*P*	n
TPiGFP into *Stat5a*$^{+/+}$	Fatal MPD: 6	31 ± 2.6	—	15
TPiGFP into *Stat5a*$^{+/-}$	Fatal MPD: 2; MPD: 5	145 ± 16.0	< .001	19
TPiGFP into *Stat5a*$^{-/-}$	Fatal MPD: 1; MPD: 8	144 ± 4.1	< .001	17
TPiStat5a add-back into *Stat5a*$^{+/-}$	Fatal MPD: 1	28 ± 9.0	.732	6
TPiStat5a add-back into *Stat5a*$^{-/-}$	Fatal MPD: 6; MPD: 2	96 ± 35.5	< .001	12
TPiStat5b add-back into *Stat5a*$^{-/-}$	MPD: 2	97 ± 7.5	< .001	8

Median survival of mice in each cohort is shown with standard error. Disease phenotype at time of death was characterized as either fatal MPD (WBC, > 50 × 10^9/L [50 000/μL] and spleen weight, > 450 mg) or MPD (WBC, > 15 × 10^9/L [15 000/μL] and/or spleen weight, > 450 mg) with number of analyzed mice indicated. Statistical significance in survival between *TPiGFP* → *Stat5*$^{+/+}$ and each cohort is shown by *P* value (determined by Mantel-Cox log rank). Statistical significance in survival between cohorts is determined by log rank (Mantel-Cox) such that the difference in survival of *TPiGFP→Stat5a*$^{-/-}$ and *TPiStat5b→Stat5a*$^{-/-}$ has a *P* value of .01 and the difference in *TPiStat5a→Stat5a*$^{-/-}$ and *TPiStat5b→Stat5a*$^{-/-}$ cohort survival has a *P* value of .79. *TPiStat5a* → *Stat5a*$^{+/-}$ mice developed severe MPD (spleen weight, 520 mg [n = 1]; WBC, 66 × 10^9/L [66 000/μL] [n = 1]). Moderate MPD was detected in *TPiStat5a* → *Stat5a*$^{-/-}$ mice (spleen weight median, 800 ± 170 mg; range, 550-970 mg [n = 8]; WBC median, 82 ± 106 × 10^9/L [82 000 ± 106 000/μL]; range, 40-108 × 10^9/L [40 000-108 000/μL] [n = 7]) and *TPiStat5b* → *Stat5a*$^{-/-}$ mice (spleen weight median, 470 ± 184 mg; range, 340-600 mg [n = 2]; WBC median, 23 ± 10 × 10^9/L [23 000 ± 10 000/μL]; range, 16-30 × 10^9/L [16 000-30 000/μL] [n = 2]). *TPiGFP* indicates *TEL-PDGFRB* ires *eGFP; TPiStat5a, TEL-PDGFRB* ires *mStat5a; TPiStat5b, TEL-PDGFRB* ires *Stat5b;* MPD, myeloproliferative disease; and WBC, peripheral white blood cell count; and —, not applicable.

Hck$^{-/-}$*Fgr*$^{-/-}$*)* (Figure 5A) developed rapidly fatal MPD characterized by elevated peripheral blood counts, extramedullary hematopoiesis, and splenomegaly (Figure 5B and data not shown). Surprisingly, coexpression of *c-Src* with *TEL-PDGFRB* to restore Src kinase activity as an add-back control was associated with longer disease latency (median survival, 71 days versus *TPiGFP→Lyn*$^{-/-}$*Hck*$^{-/-}$*Fgr*$^{-/-}$ 39 days, $P = .007$). Add-back *c-Src* may have prolonged survival of *TPiSrc→Lyn*$^{-/-}$*Hck*$^{-/-}$ *Fgr*$^{-/-}$ mice by competing with other relevant signaling molecules for binding to TEL/PDGFβR juxtamembrane tyrosines, or to other relevant signaling molecules. The development of rapidly fatal disease in *TPiGFP→Lyn*$^{-/-}$*Hck*$^{-/-}$*Fgr*$^{-/-}$ and *TPiSrc→Lyn*$^{-/-}$ *Hck*$^{-/-}$*Fgr*$^{-/-}$ mice suggests that these Src kinases are dispensable for *TEL-PDGFRB*–mediated MPD.

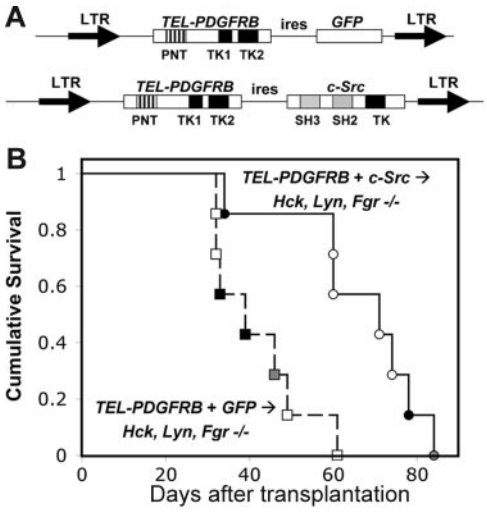

Figure 5. *TEL-PDGFRB*–mediated myeloproliferative disease does not require Src family members *Lyn, Hck,* and *Fgr.* (A) Retroviral constructs encode *TEL-PDGFRB* followed by an internal ribosomal entry site to allow expression of a second cDNA, either *GFP* or *c-Src.* (B) Kaplan-Meier plot of recipient mouse survival when *TEL-PDGFRB* is coexpressed with either GFP (□) or *c-Src* (○) in Hck-, Lyn-, and Fgr-deficient cells. The 4 *TPiGFP→Lyn*$^{-/-}$*Hck*$^{-/-}$*Fgr*$^{-/-}$ mice had varying degrees of disease severity (spleen weight, 445 ± 273 mg; range, 270-590 mg; median WBC, 38 ± 66 × 10^9/L [38 000 ± 66 000/μL]; range, 14-156 × 10^9/L [14 000-156 000/μL]). MPD was detected in 3 of 3 *TPiSrc→ Lyn*$^{-/-}$*Hck*$^{-/-}$*Fgr*$^{-/-}$ mice analyzed for disease severity at time of death (spleen weight median, 590 ± 190 mg; range, 480-850 mg; median WBC, 86 ±839 × 10^9/L [86 000 ± 839 000/μL]; range, 14-1502 × 10^9/L [14 000-1 502 000 000/μL]). Black shapes indicate death due to severe MPD marked by leukocytosis and splenomegaly (WBC, > 50 × 10^9/L [50 000/μL] and spleen weight, > 450 mg) at time of death due to disease. Shaded shapes represent moderate MPD (WBC, > 15 × 10^9/L [15 000/μL] and/or spleen weight, > 450 mg) at time of death due to disease. Open shapes indicate animal found dead. (ires indicates internal ribosomal entry site; GFP, green fluorescent protein; LTR, long terminal repeat; PNT, pointed domain; TK, tyrosine kinase; MPD, myeloproliferative disease; and WBC, peripheral white blood cell count.)

To determine the role of *Stat1* in the development of *TEL-PDGFRB*–induced MPD, we expressed *TEL-PDGFRB* in whole bone marrow harvested from *Stat1*-deficient *(TPiGFP→Stat1*$^{-/-}$*)* or wild-type control *(TPiGFP→Stat1*$^{+/+}$*)* mice. Again, all mice (100%) in both groups developed rapidly fatal MPD characterized by leukocytosis, extramedullary hematopoiesis, and splenomegaly (data not shown). *TPiGFP→Stat1*$^{-/-}$ mice developed MPD with a shorter latency than their *TPiGFP→Stat1*$^{+/+}$ counterparts (45 versus 53 days, $P = .013$), consistent with the role of Stat1 as a tumor suppressor.[30] The significantly shortened survival of *TPiGFP→Stat1*$^{-/-}$ mice indicates that Stat1 is not required for *TEL-PDGFRB* disease development. Taken together, these data demonstrate that, although TEL/PDGFβR induces both Stat5-dependent and -independent signaling, Stat5 is critical for *TEL-PDGFRB*–mediated transformation of primary hematopoietic cells.

Discussion

Using a genetic approach, we found that the signaling pathways activated by TEL/PDGFβR in cell culture do not contribute equally to transformation. The combined loss of both *Stat5a* and *Stat5b (Stat5ab*$^{null/null}$*)* eliminated *TEL-PDGFRB*–mediated transformation as measured by growth of cytokine-independent colony formation in methylcellulose (Figure 1A). Confirming the presence of hematopoietic stem and progenitor populations among *Stat5ab*$^{null/null}$ fetal liver cells, we found that they formed colonies in the presence of cytokines and that immunophenotypically-defined stem and progenitor cells were moderately increased among *Stat5ab*$^{null/null}$ over *Stat5ab*$^{+/+}$ fetal liver cells. Future comprehensive analysis of the repopulating capacity of *Stat5ab*$^{null/null}$ hematopoietic stem and progenitor cells will clarify the contribution of Stat5 to normal hematopoiesis.

Although Stat5a and Stat5b serve largely redundant functions in baseline hematopoiesis,[15,17] they made independent contributions to *TEL-PDGFRB*–mediated transformation in methylcellulose such that the loss of even a single wild-type *Stat5a* or *Stat5b* allele diminished the transformative properties of *TEL-PDGFRB,* and homozygous inactivation of either gene further reduced transformation (Figure 1B-C). The survival of *TPiGFP→Stat5a*$^{+/-}$ mice (145 ± 16 days) was closer to that of *TPiGFP→Stat5a*$^{-/-}$ mice (144 ± 4.1 days) than to *TPiGFP→Stat5a*$^{+/+}$ mice (31 ± 2.6

days). Although the normal breast development in *Stat5a*$^{+/-}$ mice[15] argues against this, we were initially concerned that undocumented expression of a truncated Stat5a protein with dominant-negative activity might explain the dramatic protection afforded *TPiGFP→Stat5a*$^{+/-}$ mice. We examined *TPiGFP→Stat5a*$^{+/-}$, *TPiGFP→Stat5a*$^{-/-}$, and *TPiGFP→Stat5a*$^{+/+}$ mice at early time points and confirmed that disease burden was tightly correlated with *Stat5a* gene dosage such that *TEL-PDGFRB*–mediated disease was sensitive to the loss of even a single wild-type *Stat5a* allele. We also addressed the concern that an underlying defect in *Stat5a*$^{-/-}$ cells might have impaired transduction and/or transplantation in our model, indirectly causing reduced sensitivity of *Stat5a*$^{+/-}$ and *Stat5a*$^{-/-}$ cells to *TEL-PDGFRB*–mediated transformation. We found that transduction efficiency was equivalent between *Stat5a*$^{-/-}$ and *Stat5a*$^{+/+}$ cells and that *Stat5*^{1*6}*→Stat5a*$^{-/-}$ recipient mice develop a rapidly fatal disease (median survival, 19 ± 1 days), indicating that Stat5a-deficient cells are transduction and transplantation competent. These data are consistent with previous results.[29]

We were surprised to find that the 2 *Stat5* genes appeared to make independent contributions to disease development in our system. In contrast to the significant decrease in myeloproliferation afforded by *Stat5a* loss, *TPiGFP→Stat5b*$^{-/-}$ mice rapidly developed fatal MPD. Unlike the uniform induction of disease in *TPiGFP→Stat5b*$^{+/+}$ mice, however, 5 of 13 *TPiGFP→Stat5b*$^{-/-}$ mice failed to develop rapidly fatal MPD (Figure 4). We repeated bone marrow transduction/transplantation experiments using *Stat5a* and *Stat5b* knock-out alleles backcrossed into the balb/c background and found similar results. Therefore, the differences in disease latency and severity we found between Stat5a and Stat5b singly deficient mice cannot be explained by differences in background strain. We performed a series of add-back experiments using *Stat5a* and *Stat5b* in a transduction/transplantation assay to confirm and compare the roles these factors play in MPD development. *Stat5a* add-back restored disease development in *TPiStat5a→Stat5a*$^{-/-}$ mice, and *Stat5b* also restored disease development when expressed in *TPiStat5b→Stat5a*$^{-/-}$ mice (Table 1). Taken together, these data suggest that our observation that the *Stat5a* and *Stat5b* genes play unequal roles in *TEL-PDGFRB*–induced MPD may be explained by exquisite sensitivity to subtle differences in Stat5a and Stat5b protein levels in different hematopoietic progenitor cells. Flow cytometric analysis of Stat5 phosphorylation will allow us to quantitatively evaluate Stat5 activation in different subsets of hematopoietic cells including stem and progenitor populations, although that work is beyond the scope of this study.

Although no signs of disease were found in *TPiGFP→Stat5a*$^{-/-}$ mice at early time points, these animals eventually succumbed to a "mild MPD" (splenomegaly with increased splenic myeloproliferation without significant peripheral leukocytosis) following a long latency (median survival, 144 days; Figure 3). The mechanism for the development of long-latency disease seen in *TPiGFP→Stat5a*$^{-/-}$ mice might be compensatory up-regulation of *Stat5b* expression or to the accumulation of additional genetic events that cooperate with TEL/PDGFβR independently of Stat5. Using *Stat5ab*$^{null/null}$ cells in a transduction and transplantation model of disease would allow us to discriminate between the consequences of Stat5-dependent and Stat5-independent signaling in *TEL-PDGFRB*–mediated disease. However, vector control–transduced *Stat5ab*$^{null/null}$ fetal liver cells were undetectable by 9 weeks after transplantation in recipient mice (data not shown), prior to the development of *TEL-PDGFRB* disease when donor fetal liver cells are used. Future transduction and transplantation studies will require alternative strategies such as conditional deletion of the *Stat5* locus in recipient mice.

While Src family kinases are activated in native PDGFβR signaling[9] and are important for S-phase induction in fibroblasts,[31] our data suggest that they are dispensable for induction of MPD by TEL/PDGFβR. Our findings are consistent with a previous report that *Lyn, Hck,* and *Fgr* are not required for myeloid disease induced by *BCR/ABL* in mice.[32] It is possible that Src activation is not functionally relevant in the context of TEL/PDGFβR due to different subcellular localization of the fusion protein and native PDGFβR. However, coexpression of *c-Src* with *TEL-PDGFRB* *(TPiSrc→Lyn*$^{-/-}$*Hck*$^{-/-}$*Fgr*$^{-/-}$*)* was associated with longer disease latency than expression of *TEL-PDGFRB* alone *(TPiGFP→Lyn*$^{-/-}$ *Hck*$^{-/-}$*Fgr*$^{-/-}$*).* Add-back *c-Src* may have competed with Stat5 at PDGFβR tyrosines 579/581, or c-Src kinase activity may have directly suppressed myeloproliferation in *TPiSrc→Lyn*$^{-/-}$*Hck*$^{-/-}$ *Fgr*$^{-/-}$ mice.[33] We considered the possibility that MPD detected in *Lyn*$^{-/-}$*Hck*$^{-/-}$*Fgr*$^{-/-}$ mice was not *TEL-PDGFRB* dependent, as Lyn and Fgr are known to have inhibitory functions,[32] but *Lyn*$^{-/-}$*Hck*$^{-/-}$*Fgr*$^{-/-}$ mice that did not undergo transplantation did not develop fatal myeloproliferation in the 3-month time frame of our experiments. While our data demonstrate that *Lyn, Hck,* and *Fgr* are not required for *TEL-PDGFRB*–mediated disease, we cannot exclude the possibility that a redundant Src family kinase was expressed in these cells and contributed in some way to disease development.

TEL/PDGFβR induces the expression of *Stat1* and multiple Stat1 target genes in Ba/F3 cells (Wilbanks et al[7]; and M.H.T., Golub, and Gilliland, unpublished data, May 2002). However, we found that *Stat1* is dispensable for *TEL-PDGFRB*–mediated disease. These data are consistent with the role of Stat1 as an antiproliferative, proapoptotic protein[30] and earlier findings that TEL/JAK2 does not require Stat1 to induce MPD or lymphoblastic lymphoma.[28]

Our data show that Stat5 plays a central role in *TEL-PDGFRB*–driven myeloproliferation. The JAK-STAT pathway is commonly activated in leukemia,[34,35] and activating JAK2 mutations have recently been discovered in association with human myeloproliferative diseases polycythemia vera (PV), essential thrombocytopenia (ET), and myeloid metaplasia and myelofibrosis (MMF) (reviewed by Tefferi and Gilliland[36]). Stat5 is required for the development of *TEL-JAK2*–induced myeloproliferative and lymphoproliferative disease in mice[28] as well as *BCR-ABL*–mediated transformation in methylcellulose colony assays.[20] Our data contribute to a model that suggests that Stat5 may be the key mediator of myeloproliferation in response to a diverse set of oncogenic tyrosine kinases.

Acknowledgments

This work was supported by NIH T32 HL07088-31A1 (J.A.C.) and NIH PO1 CA101937 (M.H.T.). This work was supported in part by the intramural program of NIDDK/NIH (L.H.).

We are grateful to C. Lowell, R. Schreiber, and H. Davey for generously providing mice harboring targeted deletion of Src and Stat family members; G. Gilliland for magnanimous support and backcross genotyping; S. Courtneidge and W. Leonard for sharing valuable reagents; T. Graubert, J. Hsieh, T. Ley, D. Link, J. Milbrandt, J. Weber, and K. Weilbaecher for valuable

discussions; and W. Eades and J. Hughes for flow cytometric progenitor analysis.

Authorship

Contribution: J.A.C. performed research (major part), designed research, and wrote the paper; Z.X. and J.O. performed research; F.K. analyzed data; A.C. performed research; L.H. provided valuable reagents; M.H.T. designed research, performed research, and wrote the paper.

Conflict-of-interest disclosure: The authors declare no competing financial interests.

Correspondence: Michael H. Tomasson, Division of Oncology, Department of Medicine, 660 S Euclid Ave, Campus Box 8007, St Louis, MO 63110; e-mail: tomasson@im.wustl.edu.

References

1. Golub TR, Barker GF, Lovett M, Gilliland DG. Fusion of PDGF receptor beta to a novel ets-like gene, tel, in chronic myelomonocytic leukemia with t(5;12) chromosomal translocation. Cell. 1994;77:307-316.
2. Carroll M, Tomasson MH, Barker GF, Golub TR, Gilliland DG. The TEL/platelet-derived growth factor beta receptor (PDGF beta R) fusion in chronic myelomonocytic leukemia is a transforming protein that self-associates and activates PDGF beta R kinase-dependent signaling pathways. Proc Natl Acad Sci U S A. 1996;93:14845-14850.
3. Jousset C, Carron C, Boureux A, et al. A domain of TEL conserved in a subset of ETS proteins defines a specific oligomerization interface essential to the mitogenic properties of the TEL-PDGFR beta oncoprotein. EMBO J. 1997;16:69-82.
4. Tran HH, Kim CA, Faham S, Siddall MC, Bowie JU. Native interface of the SAM domain polymer of TEL. BMC Struct Biol. 2002;2:5.
5. Bourgeade MF, Defachelles AS, Cayre YE. Myc is essential for transformation by TEL/platelet-derived growth factor receptor beta (PDGFRbeta). Blood. 1998;91:3333-3339.
6. Sternberg DW, Tomasson MH, Carroll M, et al. The TEL/PDGFbetaR fusion in chronic myelomonocytic leukemia signals through STAT5-dependent and STAT5-independent pathways. Blood. 2001;98:3390-3397.
7. Wilbanks AM, Mahajan S, Frank DA, Druker BJ, Gilliland DG, Carroll M. TEL/PDGFbetaR fusion protein activates STAT1 and STAT5: a common mechanism for transformation by tyrosine kinase fusion proteins. Exp Hematol. 2000;28:584-593.
8. Tomasson MH, Sternberg DW, Williams IR, et al. Fatal myeloproliferation, induced in mice by TEL/PDGFbetaR expression, depends on PDGFbetaR tyrosines 579/581. J Clin Invest. 2000;105:423-432.
9. Mori S, Ronnstrand L, Yokote K, et al. Identification of two juxtamembrane autophosphorylation sites in the PDGF beta-receptor; involvement in the interaction with Src family tyrosine kinases. EMBO J. 1993;12:2257-2264.
10. Valgeirsdottir S, Paukku K, Silvennoinen O, Heldin CH, Claesson-Welsh L. Activation of Stat5 by platelet-derived growth factor (PDGF) is dependent on phosphorylation sites in PDGF beta-receptor juxtamembrane and kinase insert domains. Oncogene. 1998;16:505-515.
11. Sachsenmaier C, Sadowski HB, Cooper JA. STAT activation by the PDGF receptor requires juxtamembrane phosphorylation sites but not Src tyrosine kinase activation. Oncogene. 1999;18:3583-3592.
12. Luo H, Li Q, O'Neal J, Kreisel F, Le Beau MM, Tomasson MH. c-Myc rapidly induces acute myeloid leukemia in mice without evidence of lymphoma-associated antiapoptotic mutations. Blood. 2005;106:2452-2461.
13. Meng F, Lowell CA. Lipopolysaccharide (LPS)-induced macrophage activation and signal transduction in the absence of Src-family kinases Hck, Fgr, and Lyn. J Exp Med. 1997;185:1661-1670.
14. Meraz MA, White JM, Sheehan KC, et al. Targeted disruption of the Stat1 gene in mice reveals unexpected physiologic specificity in the JAK-STAT signaling pathway. Cell. 1996;84:431-442.
15. Liu X, Robinson GW, Wagner KU, Garrett L, Wynshaw-Boris A, Hennighausen L. Stat5a is mandatory for adult mammary gland development and lactogenesis. Genes Dev. 1997;11:179-186.
16. Cui Y, Riedlinger G, Miyoshi K, et al. Inactivation of Stat5 in mouse mammary epithelium during pregnancy reveals distinct functions in cell proliferation, survival, and differentiation. Mol Cell Biol. 2004;24:8037-8047.
17. Udy GB, Towers RP, Snell RG, et al. Requirement of STAT5b for sexual dimorphism of body growth rates and liver gene expression. Proc Natl Acad Sci U S A. 1997;94:7239-7244.
18. Markel P, Shu P, Ebeling C, et al. Theoretical and empirical issues for marker-assisted breeding of congenic mouse strains. Nat Genet. 1997;17:280-284.
19. Traver D, Miyamoto T, Christensen J, Iwasaki-Arai J, Akashi K, Weissman IL. Fetal liver myelopoiesis occurs through distinct, prospectively isolatable progenitor subsets. Blood. 2001;98:627-635.
20. Hoelbl A, Kovacic B, Kerenyi MA, et al. Clarifying the role of Stat5 in lymphoid development and Abelson-induced transformation. Blood. 2006;107:4898-4906.
21. Yao Z, Cui Y, Watford WT, et al. Stat5a/b are essential for normal lymphoid development and differentiation. Proc Natl Acad Sci U S A. 2006;103:1000-1005.
22. Liu X, Robinson GW, Gouilleux F, Groner B, Hennighausen L. Cloning and expression of Stat5 and an additional homologue (Stat5b) involved in prolactin signal transduction in mouse mammary tissue. Proc Natl Acad Sci U S A. 1995;92:8831-8835.
23. Teglund S, McKay C, Schuetz E, et al. Stat5a and Stat5b proteins have essential and nonessential, or redundant, roles in cytokine responses. Cell. 1998;93:841-850.
24. Boucheron C, Dumon S, Santos SC, et al. A single amino acid in the DNA binding regions of STAT5A and STAT5B confers distinct DNA binding specificities. J Biol Chem. 1998;273:33936-33941.
25. Verdier F, Rabionet R, Gouilleux F, et al. A sequence of the CIS gene promoter interacts preferentially with two associated STAT5A dimers: a distinct biochemical difference between STAT5A and STAT5B. Mol Cell Biol. 1998;18:5852-5860.
26. Zhang S, Fukuda S, Lee Y, et al. Essential role of signal transducer and activator of transcription (Stat)5a but not Stat5b for Flt3-dependent signaling. J Exp Med. 2000;192:719-728.
27. Onishi M, Nosaka T, Misawa K, et al. Identification and characterization of a constitutively active STAT5 mutant that promotes cell proliferation. Mol Cell Biol. 1998;18:3871-3879.
28. Schwaller J, Parganas E, Wang D, et al. Stat5 is essential for the myelo- and lymphoproliferative disease induced by TEL/JAK2. Mol Cell. 2000;6:693-704.
29. Ye D, Wolff N, Li L, Zhang S, Ilaria RL Jr. STAT5 signaling is required for the efficient induction and maintenance of CML in mice. Blood. 2006;107:4917-4925.
30. Stephanou A, Latchman DS. Opposing actions of STAT-1 and STAT-3. Growth Factors. 2005;23:177-182.
31. Twamley-Stein GM, Pepperkok R, Ansorge W, Courtneidge SA. The Src family tyrosine kinases are required for platelet-derived growth factor-mediated signal transduction in NIH 3T3 cells. Proc Natl Acad Sci U S A. 1993;90:7696-7700.
32. Hu Y, Liu Y, Pelletier S, et al. Requirement of Src kinases Lyn, Hck and Fgr for BCR-ABL1-induced B-lymphoblastic leukemia but not chronic myeloid leukemia. Nat Genet. 2004;36:453-461.
33. Mermel CH, McLemore ML, Liu F, et al. Src family kinases are important negative regulators of G-CSF-dependent granulopoiesis. Now available as Blood. 2006;108:2562-2568.
34. Benekli M, Baer MR, Baumann H, Wetzler M. Signal transducer and activator of transcription proteins in leukemias. Blood. 2003;101:2940-2954.
35. Frohling S, Scholl C, Gilliland DG, Levine RL. Genetics of myeloid malignancies: pathogenetic and clinical implications. J Clin Oncol. 2005;23:6285-6295.
36. Tefferi A, Gilliland DG. The JAK2V617F tyrosine kinase mutation in myeloproliferative disorders: status report and immediate implications for disease classification and diagnosis. Mayo Clin Proc. 2005;80:947-958.

2007 109: 3906-3914
doi:10.1182/blood-2006-07-036335 originally published online January 11, 2007

Myeloproliferative disease induced by *TEL-PDGFRB* displays dynamic range sensitivity to *Stat5* gene dosage

Jennifer A. Cain, Zhifu Xiang, Julie O'Neal, Friederike Kreisel, AnnaLynn Colson, Hui Luo, Lothar Hennighausen and Michael H. Tomasson

Blood (print ISSN 0006-4971, online ISSN 1528-0020), is published weekly by the American Society of Hematology, 2021 L St, NW, Suite 900, Washington DC 20036.